Journal of the Brazilian Society of Mechanical Sciences and Engineering

DOI 10.1007/s40430-016-0611-x

Accepted: 24 July 2016; Published: 1 August 2016

ISSN: 1678-5878 (print version); ISSN: 1806-3691 (electronic version)

IMPACT FACTOR= 0.963

MAGNETOHYDRODYNAMIC FREE CONVECTION BOUNDARY LAYER FLOW OF NON-NEWTONIAN TANGENT HYPERBOLIC FLUID FROM A VERTICAL PERMEABLE CONE WITH VARIABLE TEMPERATURE

S. Abdul Gaffar[1], V. R. Prasad[2*], S. Keshava Reddy[1], O. Anwar Bég[3]

[1]*Department of Mathematics, Jawaharlal Nehru Technological University Anantapur, Anantapuramu - 515002,* ***India***

[2] *Department of Mathematics, Madanapalle Institute of Technology and Science, Madanapalle - 517325,* ***India***

[3] *Fluid Dynamics, Propulsion and Multi-Physics, Department of Mechanical and Aeronautical Engineering, Salford University, Newton Building, The Crescent, Salford, M54WT, England, UK.*

ABSTRACT

The nonlinear, non-isothermal steady-state boundary layer flow and heat transfer of an incompressible tangent hyperbolic non-Newtonian (viscoelastic) fluid from a vertical permeable cone with magnetic field are studied. The transformed conservation equations are solved numerically subject to physically appropriate boundary conditions using the second-order accurate implicit finite difference Keller-box technique. The numerical code is validated with previous studies. The influence of a number of emerging non-dimensional parameters, namely a Weissenberg number (We), rheological power law index (m), surface temperature exponent (n), Prandtl number (Pr), magnetic parameter (M) suction/injection parameter (f_w) and dimensionless tangential coordinate (ξ) on velocity and temperature evolution in the boundary layer regime, is examined in detail. Furthermore, the effects of these parameters on surface heat transfer rate and local skin friction are also investigated. It is observed that velocity, surface heat transfer rate and local skin friction are reduced with increasing Weissenberg number, but temperature is increased. Increasing m enhances velocity and surface heat transfer rate but reduces temperature and local skin friction. An increase in non-isothermal power law index (n) is observed to decrease the velocity and temperature. Increasing magnetic parameter (M) is found to decrease the velocity and increase the temperature. Overall, the primary influence on free convection is sustained through the magnetic body force parameter, M, and also the surface mass flux (injection/suction) parameter, f_w. The rheological effects, while still prominent, are not as dramatic. Boundary layers (both hydrodynamic and thermal) are, therefore, most strongly modified by the applied magnetic field and wall mass flux effect. The study is pertinent to smart coatings, e.g., durable paints, aerosol deposition processing and water-based solvent thermal treatment in chemical engineering.

Keywords: *Thermo-magnetohydrodynamics · Free convection · Non-Newtonian tangent hyperbolic fluid · Finite difference numerical method · Weissenberg number · Non-isothermal cone · Magnetic field*

Author for Correspondence:** ***Email – rcpmaths@gmail.com

NOMENCLATURE:

A *half angle of the cone*

B *material parameter*

B_0 *constant imposed magnetic field*

C_f *skin friction coefficient*

f *non-dimensional steam function*

f_w *Suction (wall transpiration) parameter*

Gr_x *local Grashof number*

g *acceleration due to gravity*

k *thermal conductivity of fluid*

M *magnetic parameter*

m *power law index*

n *surface temperature exponent*

Nu *heat transfer rate (Local Nusselt number)*

Pr *Prandtl number*

r *local radius of the cone*

T *temperature of the fluid*

u, v *non-dimensional velocity components along the x and y directions, respectively*

V *velocity vector*

We *Weissenberg number*

x *stream wise coordinate*

y *transverse coordinate*

Greek

α *thermal diffusivity*

β *the coefficient of thermal expansion*

ϕ *non-dimensional concentration*

η *the dimensionless radial coordinate*

μ *dynamic viscosity*

ν *kinematic viscosity*

θ *non-dimensional temperature*

ρ *density of non-Newtonian fluid*

ξ *the dimensionless tangential coordinate*

ψ *dimensionless stream function*

γ *Biot number*

Γ *Time dependent material constant*

Π *Second invariant strain tensor*

Subscripts

w *Conditions at the wall (cone surface)*

∞ *Free stream conditions*

1. INTRODUCTION

Non-Newtonian fluids have been a subject of great interest to researchers recently because of their various applications in industry and engineering. Examples of such fluids include coal-oil slurries, shampoo, paints, clay coating and suspensions, grease, cosmetic products, custard, physiological liquids (blood, bile, synovial fluid) etc. Unlike the viscous fluids, the non-Newtonian fluids cannot be described by the single constitutive relationship between the stress and the strain rate. This is due to diverse characteristics of such fluids in nature. In general, the mathematical problems in non-Newtonian fluids are more complicated because of its non-linear and higher-order than those in viscous fluids. Despite their complexities, scientists and engineers are engaged in non-Newtonian fluid dynamics. An exact solution to the viscoelastic fluid flow induced by a circular cylinder subjected to the time dependent shear stress was derived by Fetecau et al. [1]. The problems describing the unsteady helical flows of Oldroyd-B and second grade fluids were computed by Jamil et al. [2]. Tan and Masuoka [3–4] discussed the stability of the Maxwell fluid in a porous medium and derived an exact solution to the Stokes first problem for an Oldroyd-B fluid. Recent investigations include the Casson model [5], second-order Reiner-Rivlin differential fluid models [6], power-law nanoscale models [7], Eringen micro-morphic models [8], Jeffery's viscoelastic model [9] and Eyring-Powell fluid [10].

The study of non-Newtonian fluids is an important area for researchers, as the study occurs in a broad range of engineering applications, like transmission fluids, paints, transport processes in the chemical industry, storage of nuclear waste material and discoveries of the flow of oil in petroleum reservoirs. Among these non-Newtonian fluids, the tangent hyperbolic fluid [11–12] is a four-constant fluid model capable of describing shear thinning effects. The apparent viscosity varies gradually between zero shear rate and shear rate, tending to infinity. Lava, ketchup, whipped cream, blood; paints are examples of tangent hyperbolic fluid. This rheological model has certain advantages over the other non-Newtonian formulations, including simplicity, ease of computation and physical robustness. Furthermore, it is deduced from kinetic theory of liquids rather than the empirical relation. Several communications utilizing the Tangent

Hyperbolic fluid model have been presented in the scientific literature. There is no single non-Newtonian model that exhibits all the properties of non-Newtonian fluids. Hyperbolic tangent model is one of the non-Newtonian models presented by Pop and Ingham [13]. Nadeem et al. [14] made a detailed study on the peristaltic transport of a hyperbolic tangent fluid in an asymmetric channel. Recently, Nadeem and Akram [15] investigated the peristaltic flow of a MHD hyperbolic tangent fluid in a vertical asymmetric channel with heat transfer. Akram and Nadeem [16] analyzed the influence of heat and mass transfer on the peristaltic flow of a hyperbolic tangent fluid in an asymmetric channel. Akbar et al. [17] analyzed the numerical solutions of MHD boundary layer flow of tangent hyperbolic fluid on a stretching sheet. V. Ramachandra Prasad et al. [18] investigated the free convection flow and heat transfer tangent hyperbolic fluid from an isothermal sphere with partial slip effects. Very recently Prasad et al. [19] investigated the magnetohydrodynamic free convection flow and heat transfer of non-Newtonian tangent hyperbolic fluid from a horizontal circular cylinder with partial slip.

For the natural convection from cones, Hering and Grosh [20] examined the laminar free convection from a non-isothermal cone. The laminar natural convection over a frustum convection about a truncated cone was studied by Na and Chiou [21]. Yih [22] studied the effects of radiation on natural convection about a truncated cone. Pop and Na [23] examined the couple heat and mass transfer by natural convection about a truncated cone in the presence of magnetic field and radiation effects. Hossain and Paul [24] presented the free convection from a vertical permeable circular cone with non-uniform surface temperature. Ching yang cheng [25] studied the natural convection boundary layer flow of a micropolar fluid over a vertical permeable cone with variable temperature. Noghrehabadi et al. [26] examined natural convection flow of nanofluids over a vertical cone embedded in non-Darcy porous media.

Magnetohydrodynamics (MHD) refers to the study of the mutual interaction of fluid flow with magnetic fields. MHD transport phenomena arise in numerous branches of modern chemical engineering, design for cooling of nuclear reactors, construction of heat exchangers, installation of nuclear accelerators and blood flow measurement techniques. Watanabe [27-28] studied the characteristics of MHD boundary layer flow past a flat plate with/without pressure gradient. Pal and Mondal [29] examined the combined effects of thermal radiation and temperature-dependent viscosity on the momentum and heat transfer in the presence of magnetic field. Loganathan and Puvi Arasu [30] investigated the effects of thermophoresis particle deposition on the non-Darcy mixed convection heat and mass transfer past a porous wedge in the presence of suction/injection.

The objective of the present study is to investigate the laminar boundary layer flow and heat transfer of a *Tangent Hyperbolic non-Newtonian fluid* from a vertical permeable cone. The non-dimensional equations with associated dimensionless boundary conditions constitute a highly nonlinear, coupled two-point boundary value problem. Keller's implicit finite difference "box" scheme is implemented to solve the problem [5]. The effects of the emerging thermophysical parameters, namely the *Weissenberg number (We), power law index (m), surface temperature exponent (n), magnetic parameter (M), suction/injection parameter (f_w)* and *Prandtl number (Pr)* on velocity, temperature, skin friction number, and heat transfer rate (local Nusselt number) characteristics are studied. The present problem has to the authors' knowledge not appeared thus far in the scientific literature and is relevant to thermal fabrication (heat treatment) of paint sprays, water-based rheological gel solvents and low-density polymeric materials in the process engineering industry.

2. NON-NEWTONIAN CONSTITUTIVE TANGENT HYPERBOLIC FLUID MODEL

In the present study a subclass of non-Newtonian fluids known as *Tangent Hyperbolic fluid* is employed owing to its simplicity. The Cauchy stress tensor, in Tangent Hyperbolic non-Newtonian fluid [13] takes the form:

$$\bar{\tau} = \left[\mu_\infty + \left(\mu_0 + \mu_\infty \right) \tanh\left(\Gamma \bar{\dot{\gamma}} \right)^n \right] \bar{\dot{\gamma}} \tag{1}$$

where $\bar{\tau}$ is extra stress tensor, μ_∞ is the infinite shear rate viscosity, μ_0 is the zero shear rate viscosity, Γ is the time dependent material constant, m is the power law index i.e. flow behaviour index and $\bar{\dot{\gamma}}$ is defined as

$$\bar{\dot{\gamma}} = \sqrt{\frac{1}{2}\sum_i \sum_j \bar{\dot{\gamma}}_{ij} \bar{\dot{\gamma}}_{ji}} = \sqrt{\frac{1}{2}\Pi}, \tag{2}$$

Where $\Pi = \frac{1}{2} tr\left(gradV + \left(gradV \right)^T \right)^2$. We consider Eqn. (1), for the case when $\mu_\infty = 0$ because it is not possible to discuss the problem for the infinite shear rate viscosity and since we considering tangent hyperbolic fluid that describing shear thinning effects so $\Gamma \bar{\dot{\gamma}} < 1$. Then Eqn. (1) takes the form

$$\bar{\tau} = \mu_0 \left[\left(\Gamma \bar{\dot{\gamma}} \right)^n \right] \bar{\dot{\gamma}} = \mu_0 \left[\left(1 + \Gamma \bar{\dot{\gamma}} - 1 \right)^n \right] \bar{\dot{\gamma}}$$
$$= \mu_0 \left[1 + n \left(\Gamma \bar{\dot{\gamma}} - 1 \right) \right] \bar{\dot{\gamma}} \qquad (3)$$

The introduction of the appropriate terms into the flow model is considered next. The resulting boundary value problem is found to be well-posed and permits an excellent mechanism for the assessment of rheological characteristics on the flow behaviour.

3. MATHEMATICAL FLOW MODEL

Steady, laminar, two-dimensional, electrically-conducting, incompressible flow of a Tangent Hyperbolic fluid from a vertical permeable cone with variable wall temperature, as illustrated in **Fig. 1.** An induced magnetic field, B_0 is assumed to be uniform and acts radially i.e. normal to the cone surface. The origin of the coordinate system is placed at the vertex of the cone. Where x-coordinate (tangential) is measured along the surface of the cone from the origin and the y-coordinate (radial) is directed normal to the surface of the cone. Fluid suction or injection is imposed at the surface of the cone and the surface of the cone is held at a variable temperature proportional to the power of the distance i.e., $T_w(x) = T_\infty + Ad_1 x^n$. The gravitational acceleration **g**, acts downwards. Magnetic Reynolds number is assumed to be small enough to neglect magnetic induction effects. Hall current and ionslip effects are also neglected since the magnetic field is weak. We also assume that the Boussinesq approximation holds i.e. that density variation is only experienced in the buoyancy term in the momentum equation. Additionally, the electron pressure (for weakly conducting fluids) and the thermoelectric pressure are negligible. The radial magnetic field B_0 is generated by passing a steady electric current along the longitudinal (z-axis) parallel to the cone, where the cone edges terminate at perfect electrodes which are connected via a load.

Both cone and Tangent Hyperbolic fluid are maintained initially at the same temperature. Instantaneously it is raised to a temperature $T_w > T_\infty$, the ambient temperature of the fluid which remains unchanged. In line with the approach of Yih [31] and introducing the boundary layer approximations, the equations for mass, momentum, and energy, can be written as follows:

$$\frac{\partial(ru)}{\partial x} + \frac{\partial(rv)}{\partial y} = 0 \qquad (4)$$

$$u\frac{\partial u}{\partial x}+v\frac{\partial u}{\partial y}=\nu\left(1-m\right)\frac{\partial^2 u}{\partial y^2}+\sqrt{2}\nu m\Gamma\left(\frac{\partial u}{\partial y}\right)\frac{\partial^2 u}{\partial y^2}+g\beta\left(T-T_\infty\right)\cos\mathrm{A}-\frac{\sigma B_0^2}{\rho}u \tag{5}$$

$$u\frac{\partial T}{\partial x}+v\frac{\partial T}{\partial y}=\alpha\frac{\partial^2 T}{\partial y^2} \tag{6}$$

where u and v are the velocity components in the x - and y- directions respectively, $\nu=\frac{\mu}{\rho}$ - kinematic viscosity of the Tangent Hyperbolic fluid and all the other variable are defined in the nomenclature. The Tangent Hyperbolic fluid model therefore introduces a mixed derivative (second order, first degree) into the momentum boundary layer equation (5). The non-Newtonian effects feature in the shear terms only of eqn. (5) and not the convective (acceleration) terms. The third term on the right hand side of eqn. (5) represents the thermal buoyancy force and couples the velocity field with the temperature field equation (6). The fourth term on the right hand side of eqn. (5) represents the hydromagnetic drag.

$$\begin{aligned}&\text{At } y=0, \qquad u=0, \quad v=-V_w, \quad T=T_w\left(x\right)\\ &\text{As } y\to\infty, \qquad u\to 0, \quad T\to T_\infty\end{aligned} \tag{7}$$

Here n is the surface temperature exponent and d_1 is a constant, V_w is the transpiration velocity of the fluid through the surface of the cone. When V_w is positive, it stands for suction or blowing and if V_w is negative for injection or blowing of fluid through the surface of the cone. The stream function ψ is defined by $ru=\frac{\partial\psi}{\partial y}$ and $rv=-\frac{\partial\psi}{\partial x}$, and therefore, the continuity equation is automatically satisfied. Where the local radius is defined as

$$r(x) = x \sin A \tag{8}$$

In order to render the governing equations and the boundary conditions in dimensionless form, the following non-dimensional quantities are introduced.

$$\xi=\frac{V_w x}{\nu Gr^{1/4}}, \quad \eta=\frac{y}{x}Gr^{1/4}, \quad \psi=\nu r Gr^{1/4}\left(f+\frac{\xi}{2}\right), \quad \theta\left(\xi,\eta\right)=\frac{T-T_\infty}{T_w-T_\infty},$$

$$\mathrm{Pr}=\frac{\nu}{\alpha}, \quad W_e=\frac{\sqrt{2}\nu\Gamma Gr^{3/4}}{x^2}, \quad Gr=\frac{g\beta_1\left(T_w-T_\infty\right)x^3\cos A}{\nu^2}, \quad M=\frac{\sigma B_0^2 x^2}{\rho\nu Gr^{1/2}} \tag{9}$$

In view of the transformation defined in eqn. (9), the boundary layer eqns. (5) - (7) are reduced to the following coupled, nonlinear, dimensionless partial differential equations for momentum and energy for the regime:

$$(1-m)f'''+\frac{n+7}{2}ff''+\xi f''-\frac{n+1}{2}(f')^2+mW_e f''f'''-Mf'+\theta=\xi\left(\frac{1-n}{4}\right)\left(f'\frac{\partial f'}{\partial \xi}-f''\frac{\partial f}{\partial \xi}\right) \quad (10)$$

$$\frac{\theta''}{\Pr}+\frac{n+7}{4}f\theta'-nf'\theta+\xi\theta'=\xi\left(\frac{1-n}{4}\right)\left(f'\frac{\partial \theta}{\partial \xi}-\theta'\frac{\partial f}{\partial \xi}\right) \quad (11)$$

The transformed dimensionless boundary conditions are:

$$At \quad \eta=0, \quad f=f_w, \quad f'=0, \quad \theta=1$$

$$As \quad \eta\to\infty, \quad f'\to 0, \quad \theta\to 0 \quad (12)$$

Here primes denote the differentiation with respect to η and $f_w=\frac{4xV_w}{(n+7)\nu}Gr^{1/4}$. The skin-friction coefficient (shear stress at the cone surface) and Nusselt number (heat transfer rate) can be defined using the transformations described above with the following expressions.

$$Gr^{-3/4}C_f=(1-n)f''(\xi,0)+\frac{n}{2}W_e\left(f''(\xi,0)\right)^2 \quad (13)$$

$$Gr^{-1/4}Nu=-\theta'(\xi,0) \quad (14)$$

The location, ξ~ 0, corresponds to the vicinity of the lower stagnation point on the cone. For this scenario, the model defined by eqns. (10) and (11) contracts to an ordinary differential boundary value problem:

$$(1-m)f'''+\frac{n+7}{4}ff''-\frac{n+1}{2}(f')^2+mW_e f''f'''-Mf'+\theta=0 \quad (15)$$

$$\frac{\theta''}{\Pr}+\frac{n+7}{4}f\theta'-nf'\theta=0 \quad (16)$$

The general model is solved using a powerful and unconditionally stable finite difference technique introduced by Keller [32]. The Keller-box method has a second order accuracy with arbitrary spacing and attractive extrapolation features.

4. NUMERICAL SOLUTION WITH KELLER BOX IMPLICT METHOD

The Keller-Box implicit difference method is implemented to solve the nonlinear boundary value problem defined by eqns. (10) – (11) with boundary conditions (12). This technique, despite recent developments in other numerical methods, remains a powerful and very accurate approach for boundary layer flow equation systems which are generally parabolic in nature. It is unconditionally stable and achieves exceptional accuracy. An excellent summary of this technique is given in Keller [32]. Magnetohydrodynamics applications of Keller's method are reviewed in Bég [33]. This method has also been applied successfully in many rheological flow

problems in recent years. These include oblique micropolar stagnation flows [34], Walter's B viscoelastic flows [35], Stokesian couple stress flows [36], hyperbolic-tangent convection flows from curved bodies [19], micropolar nanofluids [37], Jeffrey's elasto-viscous boundary layers [38], magnetic Williamson fluids [39] and Maxwell fluids [40]. The Keller-Box discretization is fully coupled at each step which reflects the physics of parabolic systems – which are also fully coupled. Discrete calculus associated with the Keller-Box scheme has also been shown to be fundamentally different from all other mimetic (physics capturing) numerical methods, as elaborated by Keller [32]. The Keller Box Scheme comprises four stages.

1) Decomposition of the N^{th} order partial differential equation system to N first order equations.
2) Finite Difference Discretization.
3) Quasilinearization of Non-Linear Keller Algebraic Equations and finally.
4) Block-tridiagonal Elimination solution of the Linearized Keller Algebraic Equations

5. NUMERICAL RESULTS AND INTERPRETATION

Comprehensive solutions have been obtained and are presented in **Tables 1 - 3** and **Figs. 2 - 7**. The numerical problem comprises two independent variables (ξ,η), two dependent fluid dynamic variables (f,θ) and seven thermo-physical and body force control parameters, namely, We, n, m, M, Pr, f_w, ξ. The following default parameter values i.e. We = 0.3, n = 0.5, Pr = 0.71, m = 0.3, M = 0.5, f_w = 0.5, ξ = 1.0 are prescribed (unless otherwise stated). Furthermore the influence of stream-wise (transverse) coordinate on heat transfer characteristics is also investigated.

In Table 1, we compare the present results of the heat transfer rate with those obtained by Hossain and Paul [24] for natural convection heat transfer along a vertical permeable cone with variable wall temperature and are found to be in excellent agreement.

Table 2 presents the influence of the Weissenberg number (We), power law index (m), suction/injection parameter (f_w) on local skin friction and heat transfer rate, along with a variation in the transverse (stream wise) coordinate values, ξ. With increasing We, the skin friction and heat transfer rate are reduced. It is also observed that increasing m reduces skin friction but enhances heat transfer rate. And increasing f_w is found to reduce skin friction but heat transfer rate is enhanced.

Table 3 document results for the influence of surface temperature exponent (m), magnetic parameter (M), Prandtl number (Pr) on skin friction and heat transfer rate along with a variation in the traverse coordinate (ξ). It is observed that skin friction is decreased and heat transfer rate is increased with increasing m. And increasing M is found to decrease skin friction and heat

transfer rate is also decreased. Furthermore, increasing Pr, decreases skin friction but accelerates heat transfer rate.

Figures 2(a) – 2(b) depicts the effects of Weissenberg number, We on the velocity (f') and temperature (θ) distributions through the boundary layer regime. Very little tangible effect is observed in fig. 2a, although there is a very slight decrease in velocity with increase in We. Conversely, there is only a very slight increase in temperature magnitudes in fig. 2(b) with a rise in We. The mathematical model reduces to the Newtonian viscous flow model as We $\rightarrow 0$ and m $\rightarrow 0$. The momentum boundary layer equation in this case contracts to the familiar equation for Newtonian mixed convection from a cone, viz. $f'''+\frac{n+7}{4}ff''+\xi f''-\frac{n+1}{2}f'^{2}+\theta-Mf'=\xi\left(\frac{1-n}{4}\right)\left(f'\frac{\partial f'}{\partial \xi}-f''\frac{\partial f}{\partial \xi}\right)$. The thermal boundary layer equation (11) remains unchanged.

Figures 3(a) - 3(b) illustrates the effect of the power law index, m, on the velocity (f') and temperature (θ) distributions through the boundary layer regime. It is observed the the velocity is significantly increased with increasing m. Conversely, temperature is consistently reduced with increasing values of m.

Figures 4(a) – 4(b) depicts the profiles for velocity (f') and temperature (θ) for various values of the surface temperature exponent, n. It is observed that an increase in n decelerates the flow i.e., velocity decreases. Also, increasing n is found to decrease the temperature throughout the boundary layer regime.

Figures 5(a) – 5(b) depicts the profiles for velocity (f') and temperature (θ) for various values of magnetic parameter, *M*. It is observed that an increase in *M* significantly decelerates the flow i.e., velocity decreases. Conversely, increasing *M* is found to enhance the temperature. The parameter, *M*, is a Hartmann number. It simulates the relative contribution of Lorentzian magnetohydrodynamic drag force relative to viscous hydrodynamic force. As M is increased, greater opposition is generated to the flow past the cone leading to deceleration. The supplementary work expended in dragging the polymer against the imposition of the transverse magnetic field creates heating in the polymer. This dissipation of heat leads to a temperature rise and thickening of thermal boundary layers in polymers. Such phenomena are documented extensively in magnetohydrodynamic studies, for example in Makinde *et al*. [41] and Chamkha *et al*. [42].

Figures 6(a) - 6(b) shows the influence of the suction/injection parameter f_w, on the velocity (f') and temperature (θ) distributions through the boundary layer regime. It is observed that the velocity decreases significantly with increasing values of f_w, also temperature is substantially decreased with increasing f_w values.

Figures 7(a) – 7(b) depicts the velocity (f') and temperature (θ) distributions with radial coordinate, for various local suction variable, ξ. Clearly, from these figures it can be seen that as ξ increases, the maximum fluid velocity decreases. This is due to the fact that the effect of the suction is to take away the warm fluid on the cone and thereby decrease the maximum velocity with a decrease in the intensity of the natural convection rate. Fig. 7(b) shows the effect of ξ on the temperature profiles. It is noticed that the temperature profiles decrease with an increase in ξ and as the suction is increased, more warm fluid is taken away and thus the thermal boundary layer thickness decreases.

6. CONCLUSIONS

Numerical solutions have been presented for the non-similar, buoyancy-driven flow and heat transfer of Tangent Hyperbolic flow external to a vertical permeable cone. The Keller-box implicit second order accurate finite difference numerical scheme has been utilized to efficiently solve the transformed, dimensionless velocity and thermal boundary layer equations, subject to realistic boundary conditions. A comprehensive assessment of the effects of Weissenberg number (We), power law index (n), surface temperature exponent (m), magnetic body force parameter (M) and suction/injection parameter (f_w) on thermo-fluid characteristics has been conducted. Excellent correlation with previous studies has been demonstrated testifying to the validity of the present code. Generally very stable and accurate solutions are obtained with the present finite difference code. The numerical code is able to solve nonlinear boundary layer equations very efficiently and therefore shows excellent promise in simulating transport phenomena in other non-Newtonian fluids. It is therefore presently being employed to study viscoplastic fluids which also represent other chemical engineering working fluids in curved geometrical systems.

REFERENCES

[1] Fetecau, C., Mahmood, A., and Jamil, M. Exact solutions for the flow of a viscoelastic fluid induced by a circular cylinder subject to a time dependent shear stress. Communications in Nonlinear Science and Numerical Simulation, 15(12), 3931–3938 (2010)

[2] Jamil, M., Fetecau, C., and Imran, M. Unsteady helical flows of Oldroyd-B fluids. Communications in Nonlinear Science and Numerical Simulation, 16(3), 1378–1386 (2011)

[3] Tan, W. C. and Masuoka, T. Stability analysis of a Maxwell fluid in a porous medium heated from below. Physics Letters A, 360(3), 454–460 (2007)

[4] Tan, W. C. and Masuoka, T. Stokes first problem for an Oldroyd-B fluid in a porous half space. Physics of Fluids, 17(2), 023101–023107 (2005)

[5] V. Ramachandra Prasad, A Subba Rao, N Bhaskar Reddy, B Vasu and O Anwar Bég, Modelling laminar transport phenomena in a Casson rheological fluid from a horizontal circular cylinder with partial slip, Proc IMechE Part E: J Process Mechanical Engineering (2013). **DOI: 10.1177/0954408912466350**

[6] M. Norouzi, M. Davoodi, O. Anwar Bég and A.A. Joneidi, Analysis of the effect of normal stress differences on heat transfer in creeping viscoelastic Dean flow, Int. J. Thermal Sciences 69, 61-69 (2013).

[7] M. J. Uddin, N. H. M. Yusoff, O. Anwar Bég and A. I. Ismail, Lie group analysis and numerical solutions for non-Newtonian nanofluid flow in a porous medium with internal heat generation, Physica Scripta, 87 (14pp) (2013).

[8] M.M. Rashidi, M. Keimanesh, O. Anwar Bég, T.K. Hung, Magneto-hydrodynamic biorheological transport phenomena in a porous medium: A simulation of magnetic blood flow control, Int. J. Numer. Meth. Biomed. Eng. 27, 805-821 (2011)

[9] V, Ramachandra Prasad, S. Abdul gaffar, E. Keshava Reddy and O. Anwar Beg, Flow and heat transfer of Jeffery's non-Newtonian fluid from horizontal circular cylinder, Journal of Thermophysics and Heat Transfer, 28(4), 764-770, 2014

[10] V, Ramachandra Prasad, S. Abdul gaffar, E. Keshava Reddy and O. Anwar Beg, Computational study of non-Newtonian thermal convection from a vertical porous plate in a non-Darcy porous medium with Biot number effects, Journal of Porous Media, vol. 17, Issue 7, pp.601-622, 2014

[11] Noreen Sher Akbar, S. Nadeem, T. Hayat, and Awatif A. Hendi, "Effects of heat and mass transfer on the peristaltic flow of hyperbolic tangent fluid in an annulus," International Journal of Heat and Mass Transfer, vol. 54, no. 19-20, pp. 4360–4369, 2011

[12] Noreen Sher Akbar, S. Nadeem, and Mohammad Ali, Influence of heat and chemical reactions on hyperbolic tangent fluid model for blood flow through a tapered artery with a stenosis, Heat Transfer Research, 43(1)(2012)69–94.

[13]Pop, I., Ingham, D.B. Convective Heat Transfer: Mathematical and Computational Modelling of Viscous Fluids and Porous Media, Pergamon, Amsterdam, NewYork (2001).

[14] Nadeem, S., Akram, S. Peristaltic transport of a hyperbolic tangent fluid model in an asymmetric channel, ZNA, 64a (2009) 559–567.

[15] Nadeem, S., Akram, S. Magnetohydrodynamic peristaltic flow of a hyperbolic tangent fluid in a vertical asymmetric channel with heat transfer, Acta Mech. Sin., 27(2) (2011) 237–250, DOI 10.1007/s10409-011-0423-2

[16] Akram Safia, Nadeem Sohail Simulation of heat and mass transfer on peristaltic flow of hyperbolic tangent fluid in an asymmetric channel, Int. J. Numer. Meth. Fluids, (2012) DOI: 10.1002/fld.2751

[17] N S Akbar, S Nadeem. R U Haq and Z H Khan, Numerical solution of Magnetohydrodynamic boundary layer flow of tangent hyperbolic fluid towards a stretching sheet, Indian J. Phys, DOI 10.1007/s12648-013-0339-8.

[18] V, Ramachandra Prasad, S. Abdul gaffar, E. Keshava Reddy and O. Anwar Beg, Free convection flow and heat transfer tangent hyperbolic fluid from an isothermal sphere with partial slip, Arabian Journal for Science and Engineering, Vol. 39, Issue 11, pp.8157-8174, 2014

[19] V, Ramachandra Prasad, S. Abdul gaffar, E. Keshava Reddy and O. Anwar Beg, Computational analysis of magnetohydrodynamic free convection flow and heat transfer of non-Newtonian tangent hyperbolic fluid from a horizontal circular cylinder with partial slip, Int. J. of Applied and Computational Mathematics, 2015, DOI:10.1007/s40819-015-0042-x

[20] R.G. Hering, R.J. Grosh, Laminar free convection from a non-isothermal cone, International Journal of Heat and Mass Transfer 5 (1962) 1059–1068.

[21] T.Y. Na, J.P. Chiou, Laminar natural convection over a frustum of a cone, Applied Scientific Research 35 (1979) 409–421

[22] K.A. Yih, Effect of radiation on natural convection about a truncated cone, International Journal of Heat and Mass Transfer 42 (1999) 4299–4305.

[23] I. Pop, T.Y. Na, Natural convection over a vertical wavy frustum of a cone, International Journal of Non-linear Mechanics 34 (1999) 925–934.

[24] M.A. Hossain, S. C. Paul, Free convection from a vertical permeable circular cone with non-uniform surface temperature, Acta Mechanica 151 (2001) 103–114

[25] Ching-Yang Cheng, Natural convection boundary layer flow of a micropolar fluid over a vertical permeable cone with variable temperature, Int. Communications in Heat and Mass Transfer, 30, 429-433, 2011

[26] A. Noghrehabadi, A. Behseresht, M. Ghalambaz, Natural convection flow of nanofluids over a vertical cone embedded in non-Darcy porous media, Journal of Thermophysics and Heat Transfer, Vol. 27, No. 2, pp.334-341, 2013

[27] Watanabe, T., 1978. Magneto hydrodynamic stability of boundary layers along a flat plate in the presence of transverse magnetic field.ZAMM 58, 555–560

[28] Watanabe, T., 1986. Magneto hydrodynamic stability of boundary layers along a flat plate with pressure gradient. Acta Mech. 65, 41–50.

[29] Pal, D., Mondal, H., 2009. Influence of temperature-dependent viscosity and thermal radiation on MHD forced convection overa non-isothermal wedge. Appl. Math. Comput. 212, 194–208.

[30] Loganathan, P., Puvi Arasu, P., 2010. Thermophoresis effects on non-Darcy MHD mixed convective heat and mass transfer past a porous wedge in the presence of suction/injection. Theor. Appl.Mech. 37, 203–227.

[31] K.A. Yih, Viscous and Joule Heating effects on non-Darcy MHD natural convection flow over a permeable sphere in porous media with internal heat generation, International Communications in Heat and mass Transfer, 27(4), 591-600 (2000).

[32]H.B. Keller, Numerical methods in boundary-layer theory, Ann. Rev. Fluid Mech. 10, 417-433 (1978).

[33] O. Anwar Bég, Numerical methods for multi-physical magnetohydrodynamics, Chapter 1, pp. 1-112, New Developments in Hydrodynamics Research, Nova Science, New York, September (2012).

[34] Y. Y. Lok, I. Pop, D. B. Ingham, Oblique stagnation slip flow of a micropolar fluid, Meccanica, 45, 187-198 (2010).

[35] T-B. Chang, A. Mehmood, O. Anwar Bég, M. Narahari, M.N. Islam and F. Ameen, Numerical study of transient free convective mass transfer in a Walters-B viscoelastic flow with wall suction, Comm. Nonlinear Science and Numerical Simulation, 16, 216-225 (2011).

[36] D. Srinivasacharya and K. Kaladhar, Mixed convection flow of couple stress fluid in a non-Darcy porous medium with Soret and Dufour effects, J. Applied Science and Engineering, 15, 415-422 (2012).

[37] V. R. Prasad, S. A. Gaffar and O. Anwar Bég, Heat and mass transfer of a nanofluid from a horizontal cylinder to a micropolar fluid, AIAA J. Thermophysics Heat Transfer, 29, 127-139 (2015).

[38] V.R. Prasad, S. Abdul Gaffar, E. Keshava Reddy and O. Anwar Bég, Numerical study of non-Newtonian boundary layer flow of Jeffreys fluid past a vertical porous plate in a Non-Darcy porous medium, Int. J. Comp. Meth. Engineering Science & Mechanics, 15 (4) 372-389 **(2014).**

[39] R. M. Darji and M. G. Timol, On invariance analysis of MHD boundary layer equations for non-Newtonian Williamson fluids, Int. J. Adv. Appl. Math. And Mech. 1, 10 – 19 (2014)

[40] V. Singh, S. Agarwal, Flow and heat transfer of Maxwell fluid with variable viscosity and thermal conductivity over an exponentially stretching sheet, Amer. J. Fluid Dynamics, 3, 87-95 (2013). **DOI: 10.5923/j.ajfd.20130304.01**

[41] O. D. Makinde, K. Zimba, O. Anwar Bég, Numerical study of chemically-reacting hydromagnetic boundary layer flow with Soret/Dufour effects and a convective surface boundary condition, Int. J. Thermal and Environmental Engineering, 4, 89-98 (2012).

[42] A. J. Chamkha, M. Mujtaba, A. Quadri, and C. Issa, Thermal radiation effects on MHD forced convection flow adjacent to a non-isothermal wedge in the presence of a heat source or sink, Heat and Mass Transfer, 39, 305–312 (2003).

FIGURES

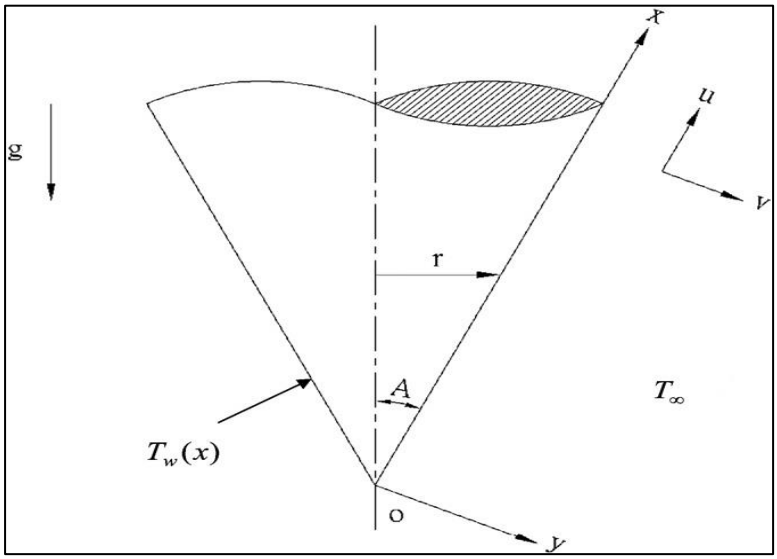

Fig. 1 Physical modal and coordinates

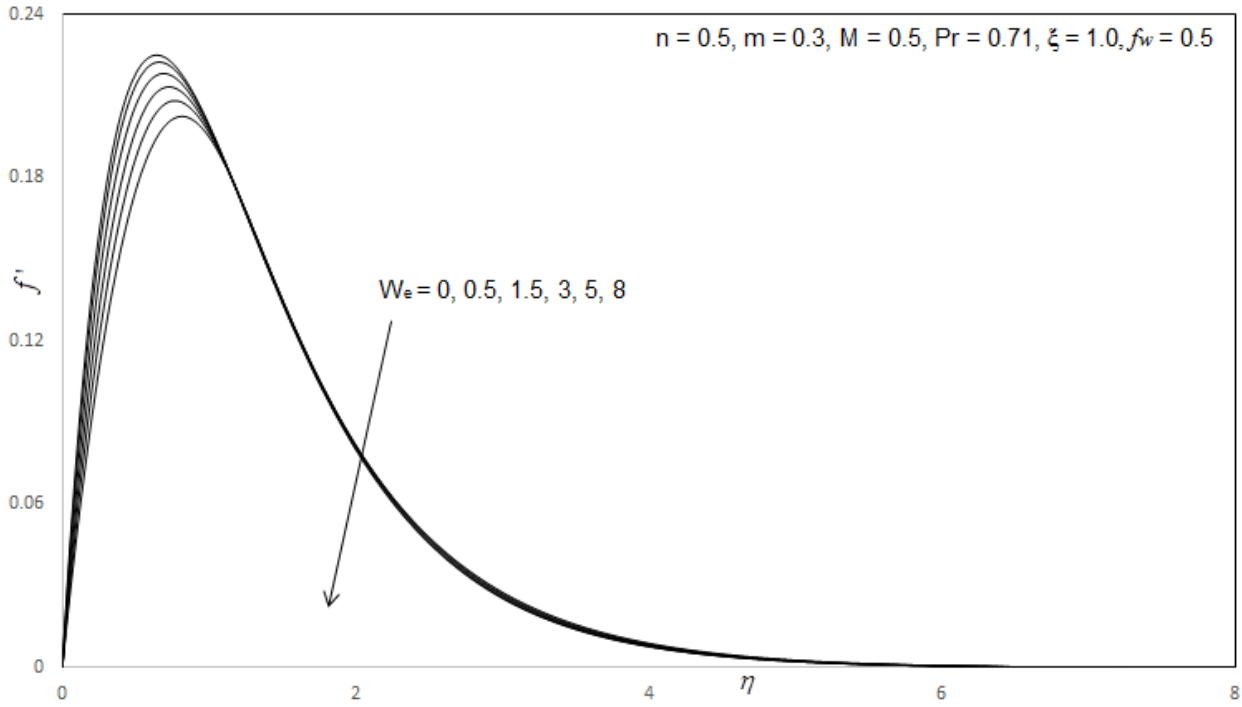

Fig. 2(a) Influence of We on Velocity Profiles

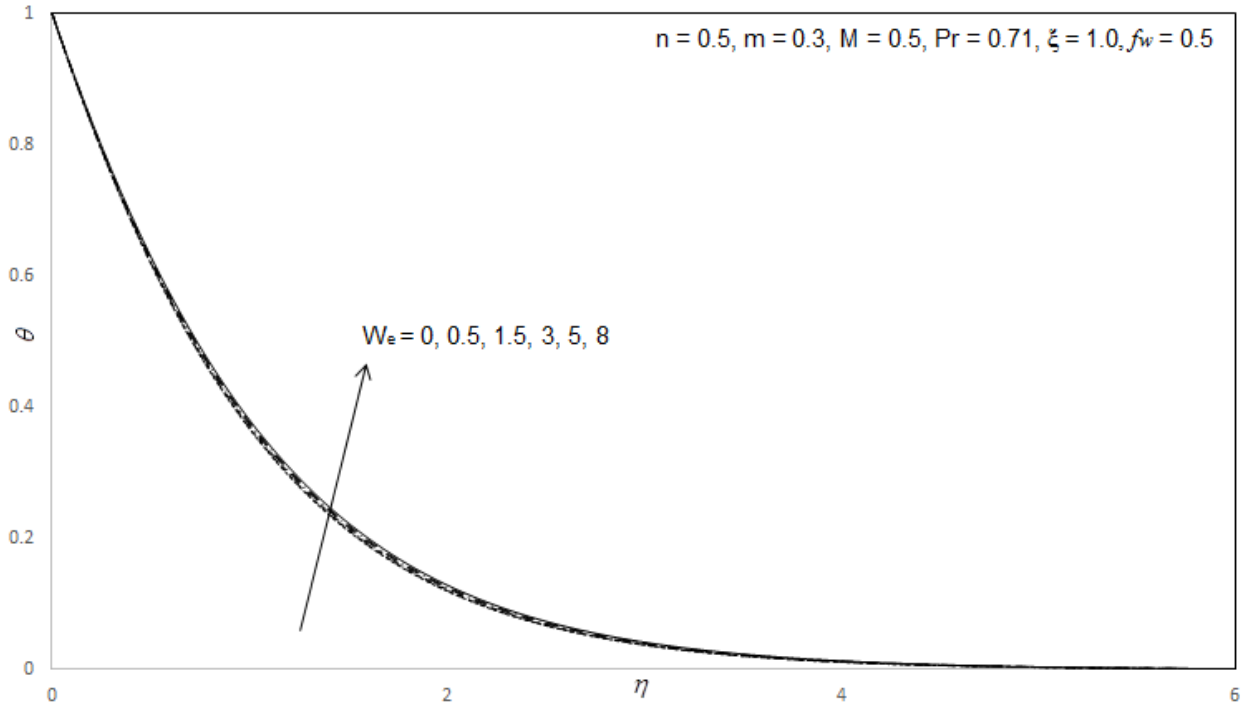

Fig. 2(b) Influence of We on Temperature Profiles

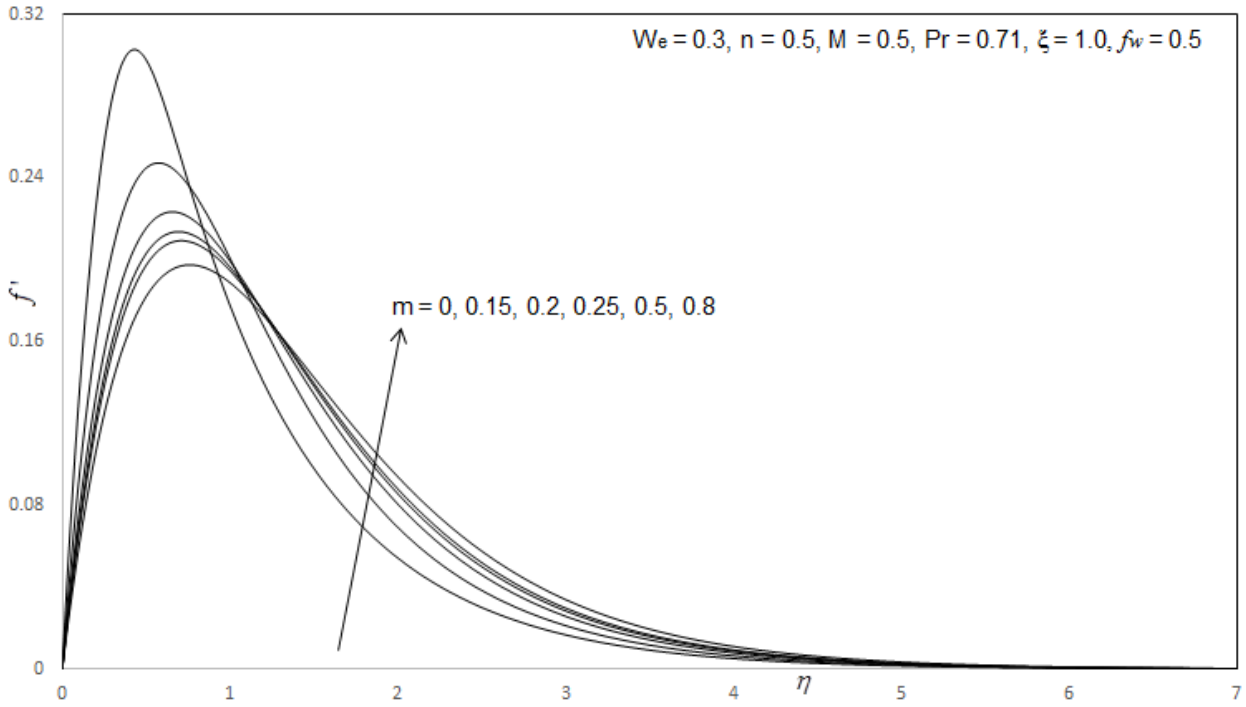

Fig. 3(a) Influence of m on Velocity Profiles

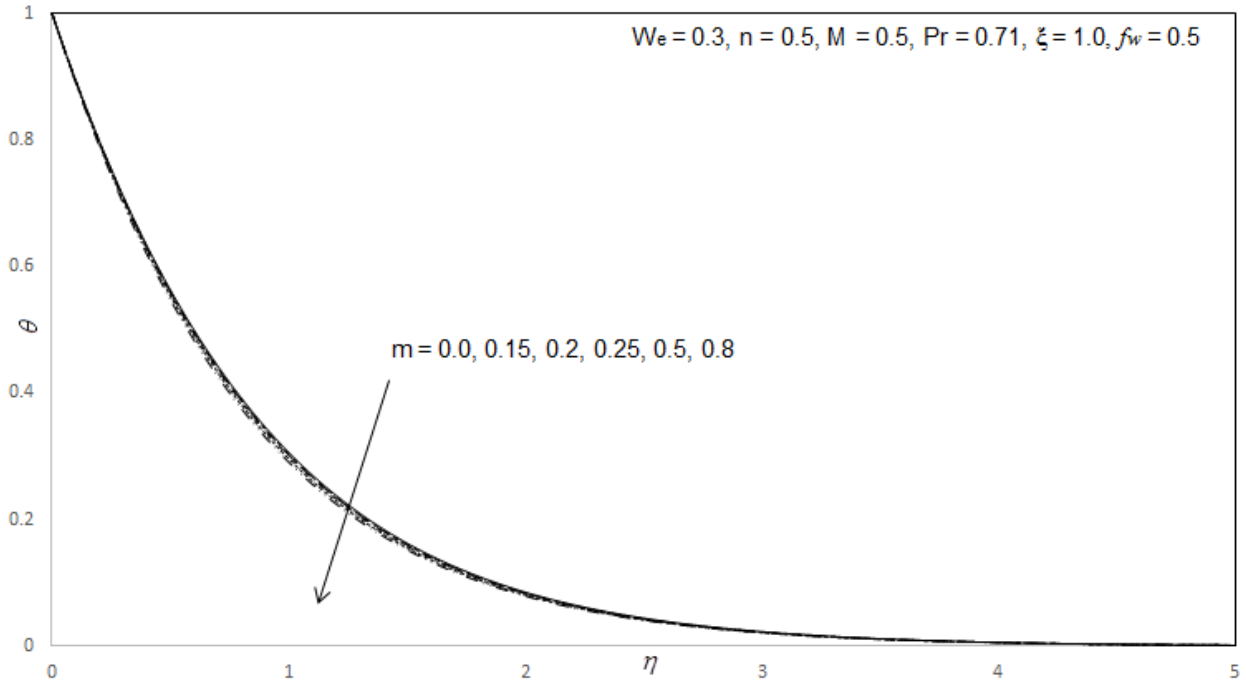

Fig. 3(b) Influence of m on Temperature Profiles

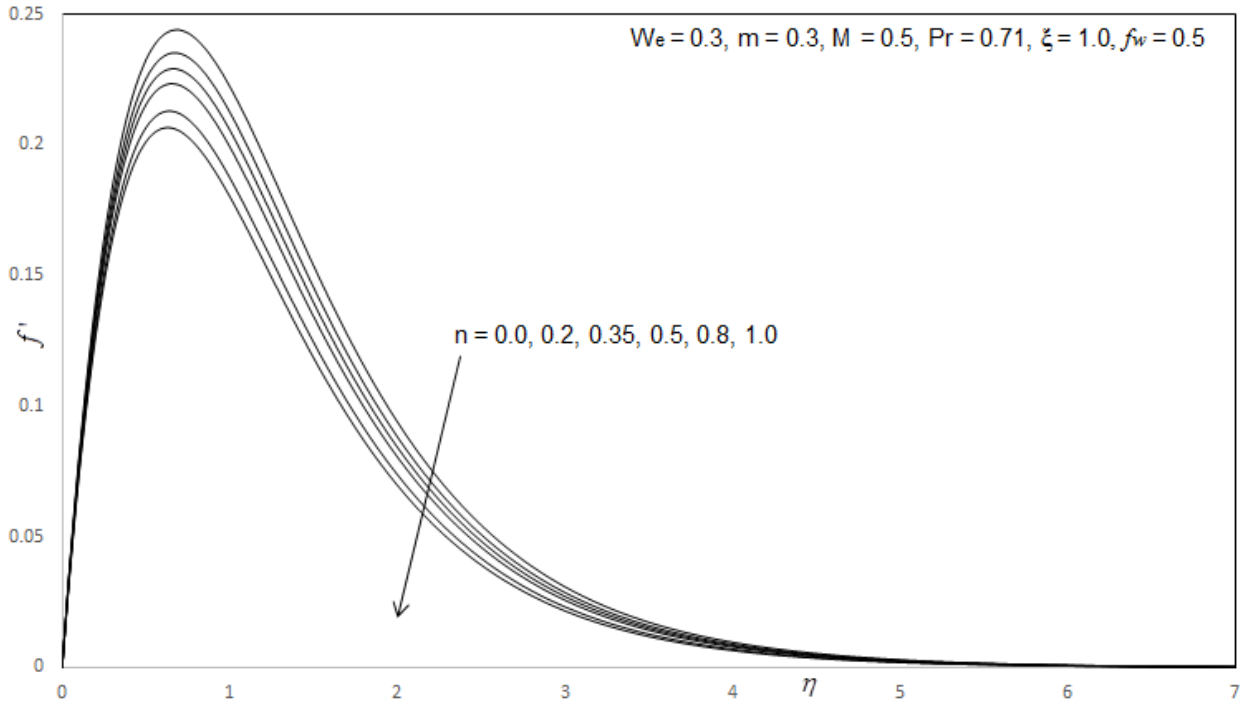

Fig. 4(a) Influence of n on Velocity Profiles

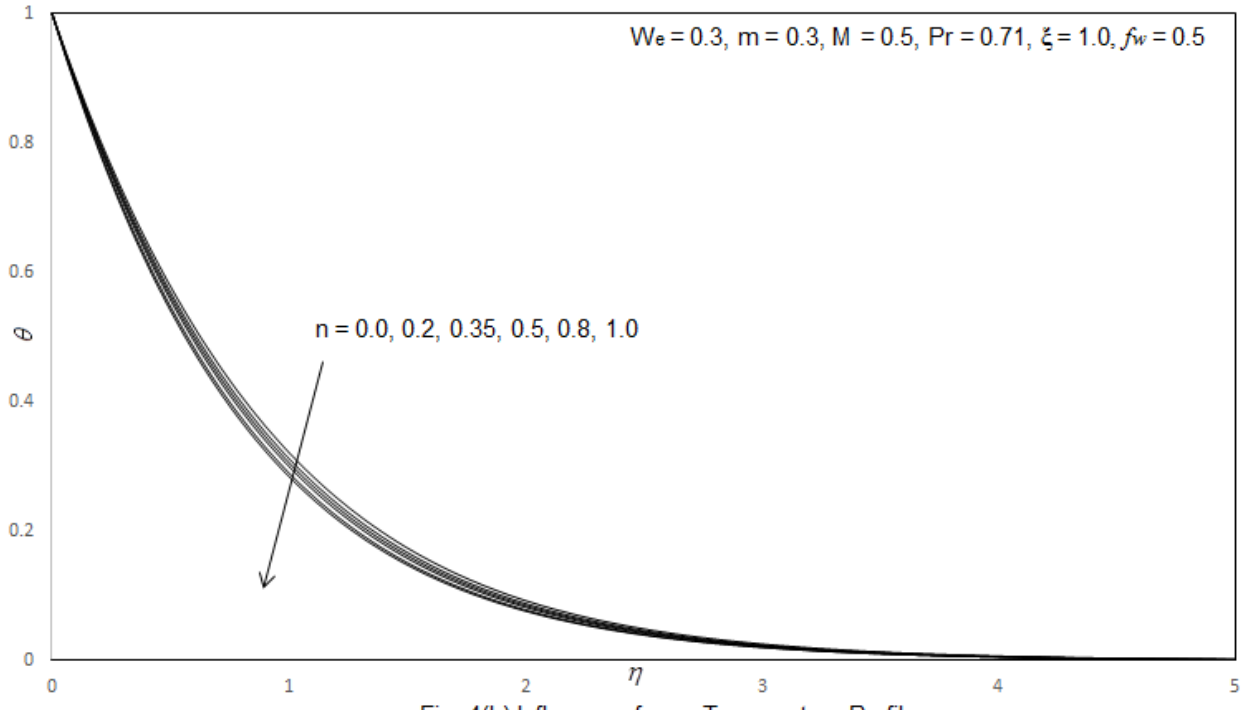

Fig. 4(b) Influence of n on Temperature Profiles

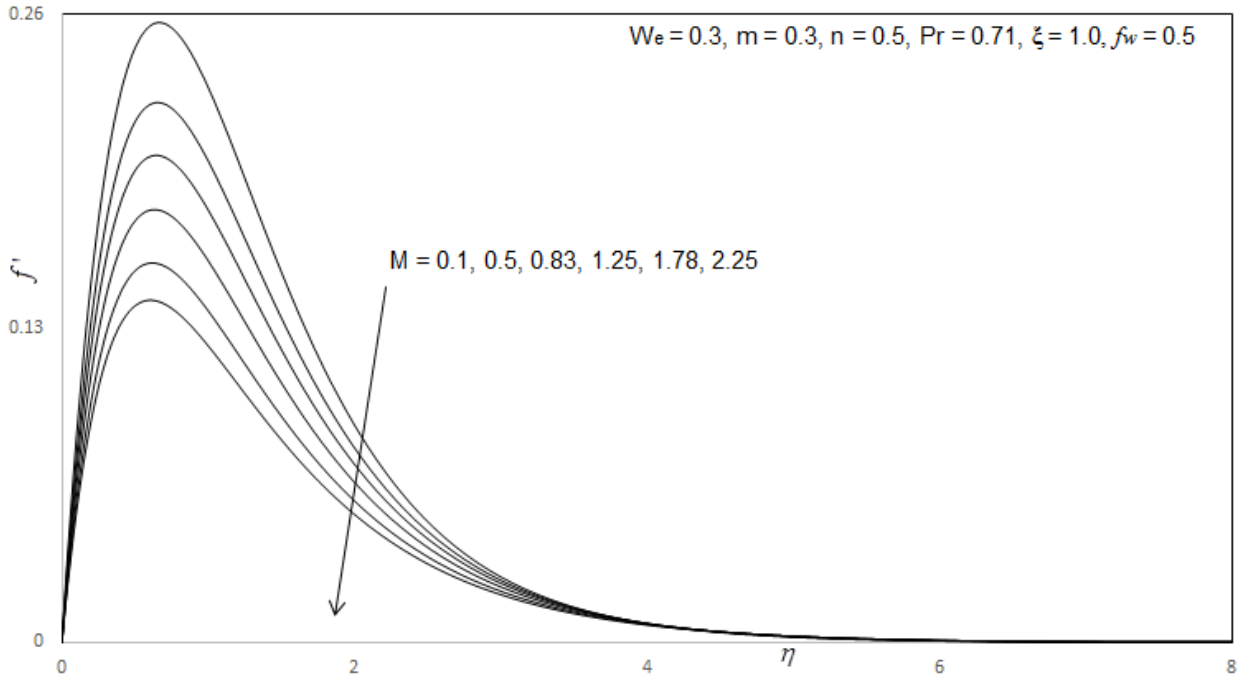

Fig. 5(a) Influence of M on Velocity Profiles

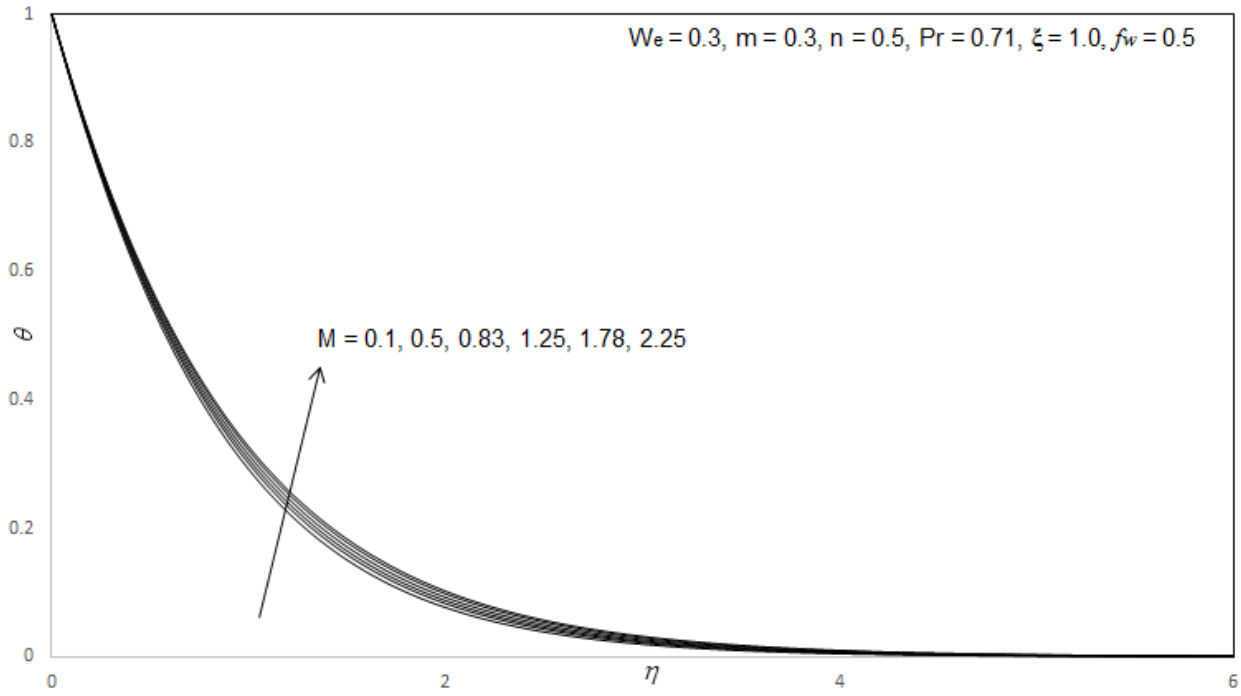

Fig. 5(b) Influence of M on Temperature Profiles

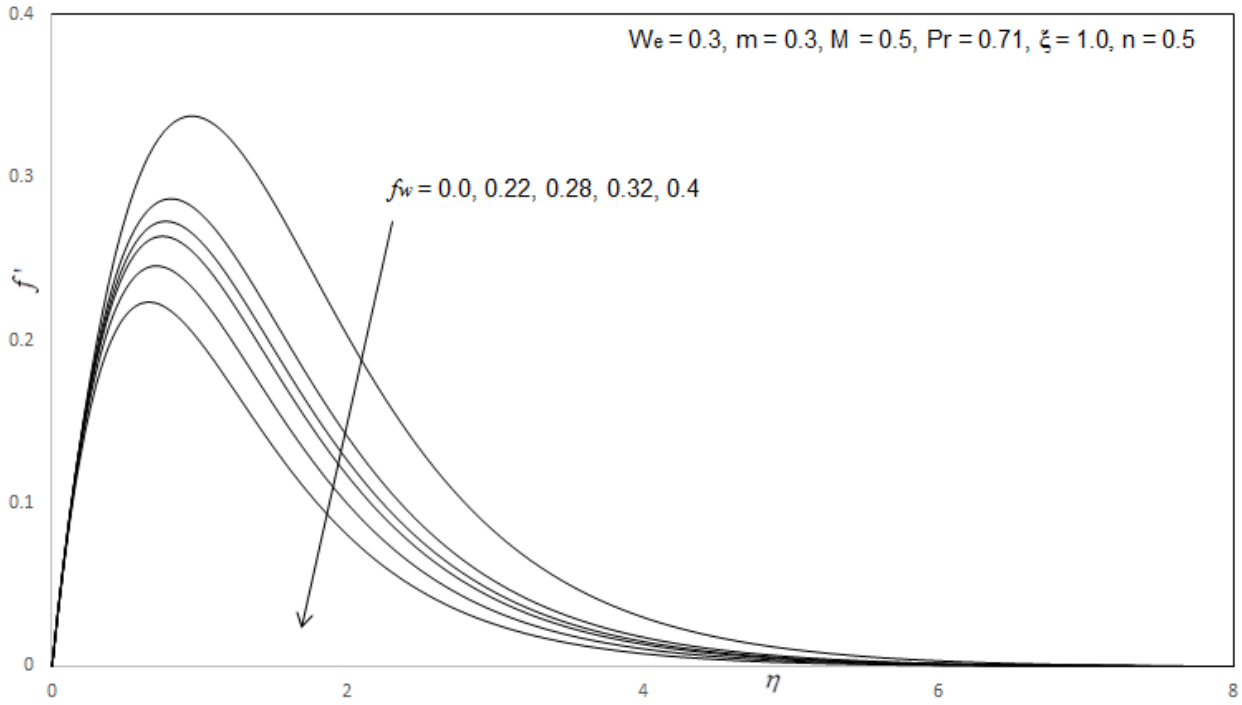

Fig. 6(a) Influence of f_w on Velocity Profiles

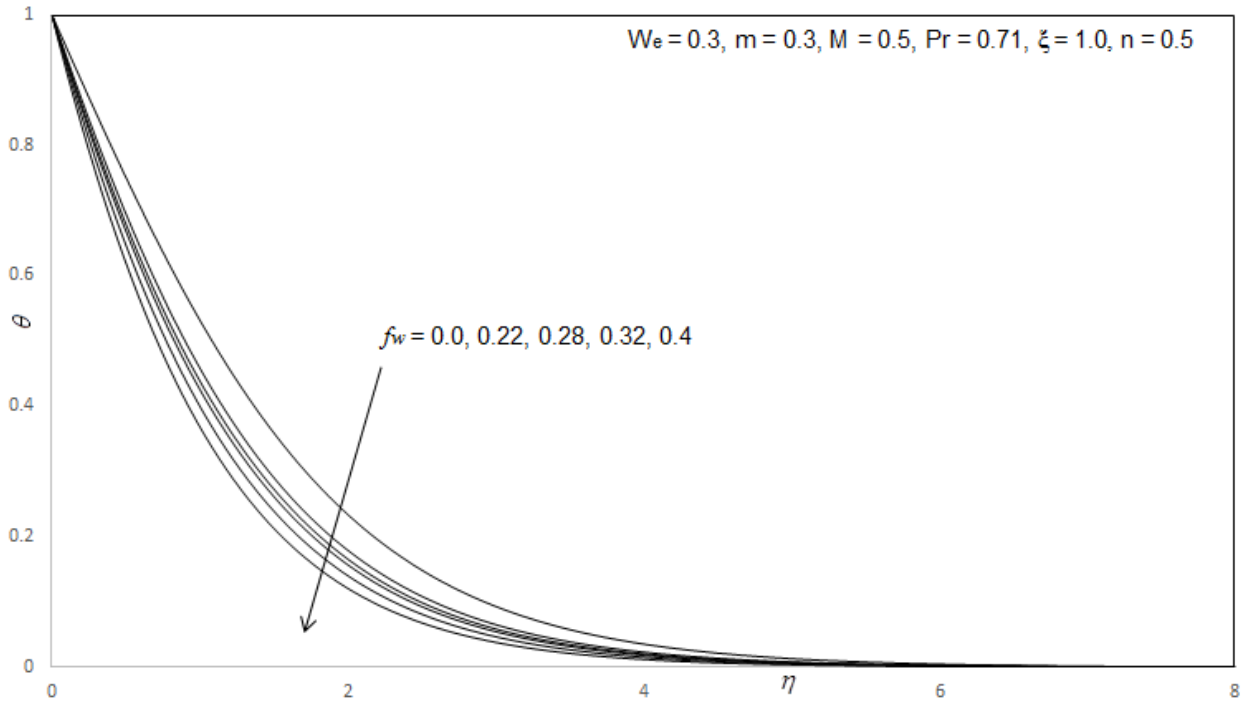

Fig. 6(b) Influence of f_w on Temperature Profiles

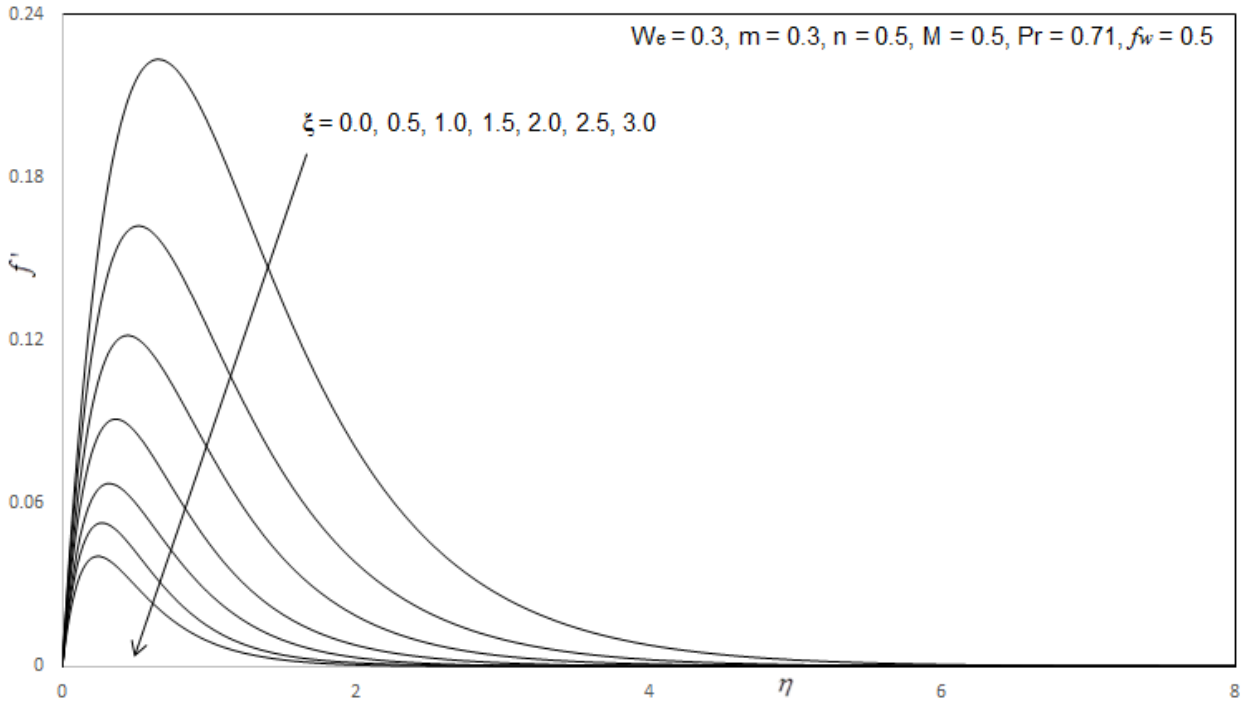

Fig. 7(a) Influence of ξ on Velocity Profiles

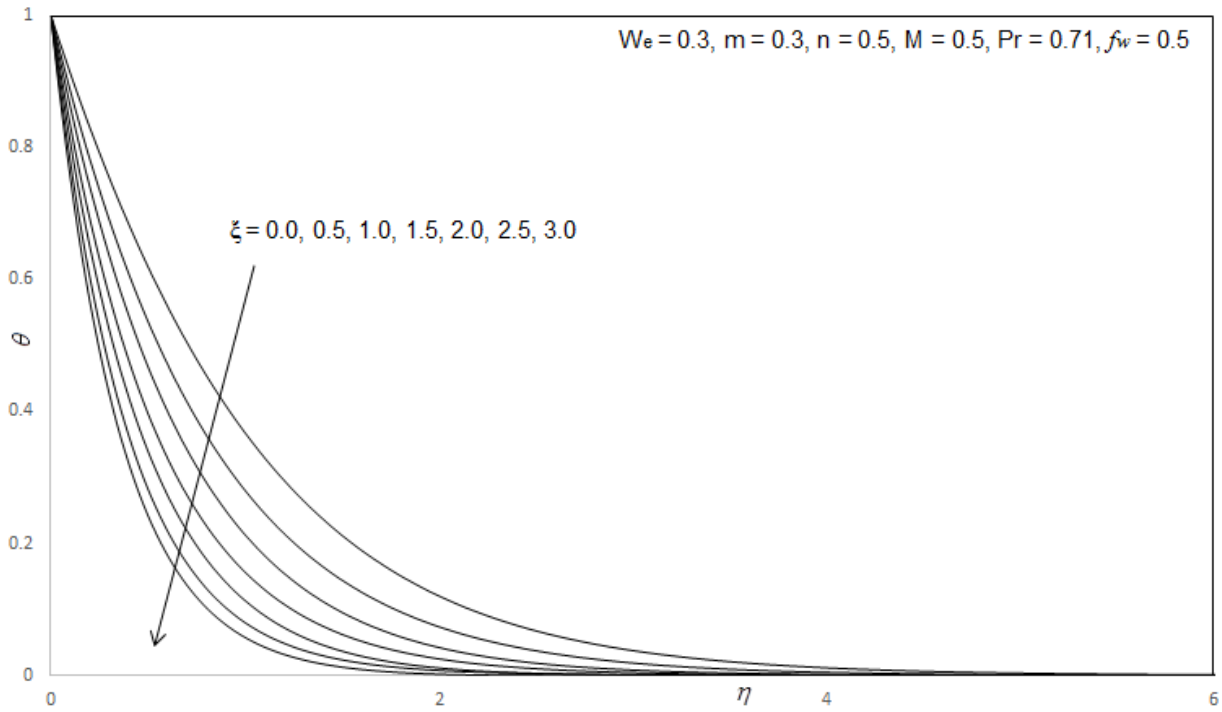

Fig. 7(b) Influence of ξ on Temperature Profiles

TABLES

Table 1: Comparison values of $-\theta'(\xi,0)$ for various values of ξ with n = 0.5, Pr = 0.1

ξ	$-\theta'(\xi,0)$	
	Hossain and Paul [18]	Present
0.0	0.24584	0.24583
0.1	0.25089	0.25087
0.2	0.25601	0.25559
0.4	0.26630	0.26631
0.6	0.27662	0.27660
0.8	0.28694	0.28692
1.0	0.29731	0.29732
2.0	0.35131	0.35132

Table 2: Values of C_f and Nu for different W_e, m and ξ (n = 0.5, A = 30^0, Pr = 071, M = 0.5)

W_e	m	f_w	ξ = 1.0		ξ = 2.0		ξ = 3.0	
			C_f	Nu	C_f	Nu	C_f	Nu
0.0	0.3	0.5	0.5349	1.4862	0.8319	2.1408	0.9843	2.8296
0.5			0.4608	1.4848	0.7388	2.1405	0.8953	2.8300
1.5			0.3561	1.4824	0.5992	2.1399	0.7550	2.8302
3.0			0.2528	1.4795	0.4545	2.1391	0.6071	2.8302
5.0			0.1620	1.4765	0.3228	2.1383	0.4565	2.8303
8.0			0.0725	1.4730	0.1896	2.1372	0.3051	2.8303
0.3	0.0	0.5	0.5450	1.4758	0.8379	2.1376	0.9883	2.8298
	0.15		0.5231	1.4803	0.8143	2.1391	0.9670	2.8299
	0.2		0.5133	1.4819	0.8031	2.1396	0.9568	2.8299
	0.5		0.4001	1.4930	0.6621	2.1430	0.8200	2.8298
	0.8		0.0432	1.5058	0.1351	2.1469	0.2838	2.8283
0.3	0.3	0.0	0.5671	0.9477	0.9697	1.5218	1.1513	2.1848
		0.22	0.5394	1.1709	0.8786	1.7882	1.0435	2.4663
		0.28	0.5295	1.2357	0.8548	1.8628	1.0170	2.5438
		0.32	0.5224	1.2798	0.8393	1.9128	0.9999	2.5956
		0.4	0.5075	1.3697	0.8092	2.0135	0.9673	2.6996
		0.45	0.4978	1.3839	0.7911	2.0769	0.9478	2.7647

Table 3: Values of C_f and Nu for different n and ξ (n = 0.5, A = 30^0, Pr = 071, M = 0.5)

N	M	Pr	ξ = 1.0		ξ = 2.0		ξ = 3.0	
			C_f	Nu	C_f	Nu	C_f	Nu
0.0	0.5	0.71	0.5064	1.4184	0.7959	2.0866	0.9496	2.7836
0.2			0.4986	1.4454	0.7871	2.1081	0.9421	2.8022
0.35			0.4932	1.4654	0.7803	2.1244	0.9356	2.8161
0.5			0.4880	1.4853	0.7735	2.1406	0.9291	2.8300
0.8			0.4832	1.5233	0.7594	2.1805	0.9103	2.8664
1.0			0.4791	1.5348	0.7385	2.1837	0.8923	2.8692
0.5	0.1	0.71	0.5259	1.4932	0.8121	2.1425	0.9585	2.8303
	0.5		0.4608	1.4853	0.7735	2.1406	0.9291	2.8300
	0.83		0.4355	1.4796	0.7919	2.1398	0.9083	2.8304
	1.25		0.4351	1.4735	0.7160	2.1389	0.8837	2.8308
	1.78		0.4064	1.4669	0.6822	2.1379	0.8551	2.8313
	2.25		0.3853	1.4617	0.6568	2.1373	0.8330	2.8321
0.5	0.5	0.5	0.5982	1.0948	1.0137	1.5315	1.2583	2.0052
		1.0	0.3863	2.0332	0.5888	2.9904	0.6791	3.9732
		2.0	0.2242	3.9541	0.3079	5.9528	0.3487	7.9486
		3.0	0.1603	5.8775	0.2176	8.9010	0.2454	11.9168
		5.0	0.1029	9.7266	0.1419	14.7524	0.1634	19.7737
		7.0	0.0756	13.5869	0.1052	20.6052	0.1225	27.6211